

## Characterization of H<sup>+</sup> and HCO<sub>3</sub><sup>-</sup> transporters in CFPAC-1 human pancreatic duct cells

Zoltán Rakonczay Jr, Amy Fearn, Péter Hegyi, Imre Boros, Michael A Gray, Barry E Argent

Zoltán Rakonczay Jr, Amy Fearn, Péter Hegyi, Michael A Gray, Barry E Argent, Institute for Cell and Molecular Biosciences, University of Newcastle upon Tyne, Medical School, Newcastle upon Tyne NE2 4HH, United Kingdom

Zoltán Rakonczay Jr, Péter Hegyi, First Department of Medicine, Faculty of Medicine, University of Szeged, H-6720 Szeged, Hungary

Imre Boros, Hungarian Academy of Sciences, Biological Research Center, Institute of Biochemistry, H-6726 Szeged, Hungary

Supported by a Wellcome Trust Travelling Fellowship to Z.R., No. 069470, and a Wellcome Trust IRDA Grant to P.H., No. 068096

Correspondence to: Professor Barry E Argent, Institute for Cell and Molecular Biosciences, University of Newcastle upon Tyne, Medical School, Framlington Place, Newcastle upon Tyne NE2 4HH, United Kingdom. b.e.argent@ncl.ac.uk

Telephone: +44-191-222-7009 Fax: +44-191-222-7424

Received: 2005-07-18

Accepted: 2005-08-03

### Abstract

**AIM:** To characterize H<sup>+</sup> and HCO<sub>3</sub><sup>-</sup> transporters in polarized CFPAC-1 human pancreatic duct cells, which were derived from a cystic fibrosis patient with the ΔF508 CFTR mutation.

**METHODS:** CFPAC-1 cells were seeded at high density onto permeable supports and grown to confluence. The cells were loaded with the pH-sensitive fluorescent dye BCECF, and mounted into a perfusion chamber, which allowed the simultaneous perfusion of the basolateral and apical membranes. Transmembrane base flux was calculated from the changes in intracellular pH and the buffering capacity of the cells.

**RESULTS:** Our results showed differential permeability to HCO<sub>3</sub><sup>-</sup>/CO<sub>2</sub> at the apical and basolateral membranes of CFPAC-1 cells. Na<sup>+</sup>/HCO<sub>3</sub><sup>-</sup> co-transporters (NBCs) and Cl<sup>-</sup>/HCO<sub>3</sub><sup>-</sup> exchangers (AEs) were present on the basolateral membrane, and Na<sup>+</sup>/H<sup>+</sup> exchangers (NHEs) on both the apical and basolateral membranes of the cells. Basolateral HCO<sub>3</sub><sup>-</sup> uptake was sensitive to variations of extracellular K<sup>+</sup> concentration, the membrane permeable carbonic anhydrase (CA) inhibitors acetazolamide (100 μmol/L) and ethoxzolamide (100 μmol/L), and was partially inhibited by H<sub>2</sub>-DIDS (600 μmol/L). The membrane-impermeable CA inhibitor 1-*N*-(4-sulfamoylphenylethyl)-2,4,6-trimethylpyridine perchlorate did not have any effect on HCO<sub>3</sub><sup>-</sup> uptake.

The basolateral AE had a much higher activity than that in the apical membrane, whereas there was no such difference with the NHE under resting conditions. Also, 10 μmol/L forskolin did not significantly influence Cl<sup>-</sup>/HCO<sub>3</sub><sup>-</sup> exchange on the apical and basolateral membranes. The administration of 250 μmol/L H<sub>2</sub>-DIDS significantly inhibited the basolateral AE. Amiloride (300 μmol/L) completely inhibited NHEs on both membranes of the cells. RT-PCR revealed the expression of pNBC1, AE2, and NHE1 mRNA.

**CONCLUSION:** These data suggest that apart from the lack of CFTR and apical Cl<sup>-</sup>/HCO<sub>3</sub><sup>-</sup> exchanger activity, CFPAC-1 cells express similar H<sup>+</sup> and HCO<sub>3</sub><sup>-</sup> transporters to those observed in native animal tissue.

© 2006 The WJG Press. All rights reserved.

**Key words:** CFPAC-1; Pancreatic duct cells; HCO<sub>3</sub><sup>-</sup>; Intracellular pH

Rakonczay Z Jr, Fearn A, Hegyi P, Boros I, Gray MA, Argent BE. Characterization of H<sup>+</sup> and HCO<sub>3</sub><sup>-</sup> transporters in CFPAC-1 human pancreatic duct cells. *World J Gastroenterol* 2006; 12(6): 885-895

<http://www.wjgnet.com/1007-9327/12/885.asp>

### INTRODUCTION

There are two HCO<sub>3</sub><sup>-</sup> transport processes in the pancreatic ductal epithelium. The first is the secretion, mainly by the smaller ducts, of HCO<sub>3</sub><sup>-</sup> rich isotonic fluid that serves to flush digestive enzymes down the ductal tree and to neutralize gastric acid entering the duodenum<sup>[1,2]</sup>. The second HCO<sub>3</sub><sup>-</sup> transport process is the flow-dependent exchange of luminal HCO<sub>3</sub><sup>-</sup> for blood Cl<sup>-</sup> that is generally considered to occur in the larger ducts, including the main duct<sup>[1,2]</sup>. The physiological function of ductal HCO<sub>3</sub><sup>-</sup> absorption (or salvage) may be protective as it will lower luminal HCO<sub>3</sub><sup>-</sup> (and therefore luminal pH) during interdigestive periods when the flow is low or absent. A fall in luminal pH would reduce the activity of digestive enzymes within the static column of fluid in the ductal tree, thereby preventing damage to the ductal epithelium.

The initial step of HCO<sub>3</sub><sup>-</sup> secretion is the accumulation of HCO<sub>3</sub><sup>-</sup> within the duct cell<sup>[1,2]</sup>. This can occur by two

mechanisms: (1) the forward transport of  $\text{HCO}_3^-$  by the  $\text{Na}^+/\text{HCO}_3^-$  co-transporter (NBC); and (2) diffusion of  $\text{CO}_2$  into the duct cell which is then hydrated to carbonic acid by carbonic anhydrase (CA), followed by the backward transport of protons via the  $\text{Na}^+/\text{H}^+$  exchangers and  $\text{H}^+$ -pumps. The  $\text{HCO}_3^-$  ions are then secreted across the apical membrane via  $\text{Cl}^-/\text{HCO}_3^-$  exchangers (SLC26A3, DRA and SLC26A6, PAT1)<sup>[3]</sup> and/or cystic fibrosis transmembrane conductance regulator (CFTR)  $\text{Cl}^-$  channels, which exhibit a finite permeability to  $\text{HCO}_3^-$ <sup>[4,5]</sup>. The exact mechanism how the SLC26 exchangers and apical  $\text{Cl}^-$  channels produce a high  $\text{HCO}_3^-$  secretion is controversial<sup>[1,2]</sup>. Nevertheless, the key role of CFTR in  $\text{HCO}_3^-$  secretion is emphasized by the fact that the severity of the pancreatic phenotype in cystic fibrosis correlates best with the ability of mutant CFTRs to activate SLC26 exchangers, rather than their ability to conduct  $\text{Cl}^-$  ions<sup>[6]</sup>.

Rather less is known about the secondary, flow- and  $\text{Cl}^-$ -dependent absorption of  $\text{HCO}_3^-$  that occurs in the larger ducts. A luminal  $\text{Na}^+/\text{H}^+$  exchanger (NHE3) and an electroneutral NBC (SLC4A7, NBCn1, NBC3) have been identified in the main duct of the mouse pancreas and probably explain  $\text{HCO}_3^-$  absorption across the apical membrane<sup>[7-9]</sup>. There is a clear evidence that activity of these luminal  $\text{HCO}_3^-$  salvage transporters is downregulated following stimulation of  $\text{HCO}_3^-$  secretion by a rise in intracellular cyclic AMP<sup>[7-9]</sup>. How the absorbed  $\text{HCO}_3^-$  exits the duct cell at the basolateral membrane is uncertain, but a candidate pathway is the basolateral  $\text{Cl}^-/\text{HCO}_3^-$  exchanger (possibly AE2)<sup>[10]</sup>. The AE2 must be switched off during stimulation as the prevailing ion gradients would favor  $\text{Cl}^-$  uptake and  $\text{HCO}_3^-$  efflux across the basolateral membrane.

Our current understanding of pancreatic ductal  $\text{HCO}_3^-$  secretion/salvage is mainly based on the experiments performed in animal tissues<sup>[1]</sup>. Studies in human tissue have been largely confined to adenocarcinoma duct cell lines; however, with the exception of CAPAN-1, human duct cell lines do not express CFTR to any significant degree<sup>[11]</sup>. An alternative approach is to use CFPAC-1 cells, which were derived from a 26-year-old cystic fibrosis (CF) patient with the  $\Delta\text{F508}$  mutation<sup>[12]</sup>. The utility of CFPAC-1 cells is that they allow us to examine  $\text{HCO}_3^-$  transport not only in the diseased state, but also in the corrected state by transfecting the cells with wild-type CFTR. A number of previous studies have shown that wild-type CFPAC-1 cells express some of the key transporters involved in  $\text{HCO}_3^-$  secretion; e.g. the basolateral NBC<sup>[13]</sup>, anion exchanger-2 and the apical  $\text{Cl}^-/\text{HCO}_3^-$  exchangers DRA and PAT-1<sup>[14]</sup>. Moreover, the expression of apical  $\text{Cl}^-/\text{HCO}_3^-$  exchangers was significantly increased in CFPAC-1 cells expressing functional CFTR, as was the stimulatory effect of ATP on luminal  $\text{Cl}^-/\text{HCO}_3^-$  exchange<sup>[15]</sup>. CFPAC-1 cells can also be reconstituted as polarized monolayers on permeable supports and the effects of various agents, such as angiotensin II<sup>[16,17]</sup> and PKC<sup>[18]</sup>, have been studied using the short circuit current technique. Finally, in one study a stimulatory effect of ATP on  $\text{HCO}_3^-$  secretion from CFPAC cells was demonstrated by measuring the extracellular pH at the apical cell surface<sup>[19]</sup>.

A number of issues regarding the mechanism of pancreatic ductal  $\text{HCO}_3^-$  secretion remain controversial.

For instance, how much of the secreted  $\text{HCO}_3^-$  enters the lumen via CFTR and how much via SLC26 anion exchangers? How is coordinate regulation of apical and basolateral acid base transporters achieved during secretion and salvage? How do luminal signals regulate apical  $\text{HCO}_3^-$  and  $\text{H}^+$  transporters? What is the molecular explanation for the strong outward rectification of  $\text{HCO}_3^-$  permeability exhibited by the apical membrane of the duct cell? A human pancreatic duct cell line, which reconstituted as a polarized monolayer allowing easy access to the luminal membrane, would be a very useful resource for answering these questions. An added bonus would be a model system that facilitates investigation of how CFTR expression affects duct cell transporters. Therefore, in this study, we aimed to establish whether polarized CFPAC-1 cells grown on permeable supports could fulfill these requirements. To do this, we investigated the  $\text{HCO}_3^-$  permeability characteristics of the basolateral and apical membranes of CFPAC-1 cells, and the spatial distribution of acid/base transporters.

## MATERIALS AND METHODS

### Materials and solutions

All laboratory chemicals were purchased from Sigma (Poole, Dorset, UK). 2',7'-Bis-(2-carboxyethyl)-5(6)-carboxyfluorescein-acetoxymethyl ester (BCECF-AM) and dihydro-4,4'-diisothiocyanostilbene-2,2'-disulfonic acid ( $\text{H}_2\text{-DIDS}$ ) were from Molecular Probes Inc. (Eugene, OR, USA); 1-*N*-(4-sulfamoylphenylethyl)-2,4,6-trimethylpyridine perchlorate (STP) was kindly provided by Prof. C Supuran. Stock solutions of BCECF (2 mmol/L), acetazolamide (0.4 mol/L), ethoxzolamide (0.4 mol/L), amiloride (0.8 mol/L) and STP (10 mmol/L) were prepared in dimethyl sulfoxide (DMSO). Nigericin (10 mmol/L) and forskolin (50 mmol/L) were dissolved in ethanol and stored at  $-20^\circ\text{C}$ . Polyester Transwells were supplied by Corning-Costar (Buckinghamshire, UK). The standard HEPES-buffered solution contained 130 mmol/L NaCl, 5 mmol/L KCl, 1 mmol/L  $\text{MgCl}_2$ , 1 mmol/L  $\text{CaCl}_2$ , 10 mmol/L Na-HEPES, and 10 mmol/L D-glucose (pH 7.4 with HCl). In the  $\text{Na}^+$ -free HEPES solution, NaCl was replaced by 140 mmol/L *N*-methyl-D-glucamine (NMDG)-Cl and the Na-HEPES was replaced by equimolar HEPES-acid. The  $\text{Cl}^-$ -free HEPES solution contained 140 mmol/L Na-gluconate, 2.5 mmol/L  $\text{K}_2\text{SO}_4$ , 6 mmol/L Ca-gluconate, 1 mmol/L Mg-gluconate, 10 mmol/L HEPES-acid, 10 mmol/L D-glucose (pH 7.4 with NaOH). The  $\text{Na}^+/\text{Cl}^-$ -free HEPES solution contained 130 mmol/L NMDG-gluconate, 2.5 mmol/L  $\text{K}_2\text{SO}_4$ , 1 mmol/L  $\text{MgSO}_4$ , 1 mmol/L  $\text{CaSO}_4$ , 10 mmol/L HEPES-acid, 10 mmol/L D-glucose (pH 7.4 with gluconate). The standard  $\text{HCO}_3^-$  solution contained 115 mmol/L NaCl, 5 mmol/L KCl, 1 mmol/L  $\text{MgCl}_2$ , 1 mmol/L  $\text{CaCl}_2$ , 25 mmol/L Na- $\text{HCO}_3$ , 10 mmol/L D-glucose. In the  $\text{K}^+$ -free  $\text{HCO}_3^-$  solution, KCl was replaced with equimolar NaCl. The high  $\text{K}^+$   $\text{HCO}_3^-$  solution contained the same ingredients as the standard  $\text{HCO}_3^-$  solution but the KCl and NaCl concentrations were 115 and 5 mmol/L, respectively. The  $\text{Na}^+$ -free  $\text{HCO}_3^-$  solution contained NMDG-Cl instead of NaCl and choline  $\text{HCO}_3^-$  in place of  $\text{NaHCO}_3$ .  $\text{Cl}^-$ -free

HCO<sub>3</sub><sup>-</sup> solution contained 115 mmol/L sodium gluconate, 2.5 mmol/L K<sub>2</sub>SO<sub>4</sub>, 6 mmol/L Ca-gluconate, 1 mmol/L Mg-gluconate, 25 mmol/L Na-HCO<sub>3</sub>, 10 mmol/L D-glucose. The Na<sup>+</sup>/Cl<sup>-</sup>-free HCO<sub>3</sub><sup>-</sup> solution contained 115 mmol/L NMDG-gluconate, 2.5 mmol/L K<sub>2</sub>SO<sub>4</sub>, 1 mmol/L MgSO<sub>4</sub>, 1 mmol/L CaSO<sub>4</sub>, 25 mmol/L choline-HCO<sub>3</sub><sup>-</sup>, 10 mmol/L D-glucose (pH 7.4 with gluconate). 10 μmol/L atropine was added to the solutions containing choline to prevent the possible activation of muscarinic receptors. In solutions containing NH<sub>4</sub><sup>+</sup>, the concentration of Na<sup>+</sup> or NMDG was replaced to maintain osmolarity. All the solutions containing HCO<sub>3</sub><sup>-</sup> were continuously equilibrated with 5% CO<sub>2</sub>-95% O<sub>2</sub> to maintain pH at 7.4.

### Culture of CFPAC-1 cells

CFPAC-1 cells (passage number 27-60) were obtained from Prof. RA Frizzell (University of Pittsburgh, Pittsburgh, PA, USA) and were grown in Iscove's modified Dulbecco's medium supplemented with 100 mL/L fetal calf serum, 2 mmol/L glutamine, 100 units/mL penicillin and 0.1 mg/mL streptomycin and were cultured as described previously<sup>[12]</sup>. The media was changed every 1-2 d. Cells were maintained at 37 °C in a humidified atmosphere containing 5% CO<sub>2</sub>. Cell monolayers were prepared by seeding at high density (300-350 cells/cm<sup>2</sup>) onto polyester permeable supports (12 mm diameter, 0.4 μm pore size Transwells). Cell confluence was checked by microscopy and determination of transepithelial electrical resistance using an EVOM-G voltohmmeter (World Precision Instruments, Sarasota, FL, USA). Experiments were performed 4-6 d after seeding.

### Measurement of intracellular pH

Intracellular pH<sub>i</sub> was estimated with the pH-sensitive dye BCECF<sup>[20,21]</sup>. CFPAC-1 cells were loaded with 2 μmol/L BCECF-AM in both the apical and basal chambers in standard HEPES for 30-45 min at 37 °C. After loading, the Transwells were transferred to a perfusion chamber mounted on an inverted Nikon Diaphot microscope (Nikon UK, Kingston upon Thames, UK). Apical and basal bath volumes were 0.5 and 1 mL and the perfusion rates were 3 and 6 mL/min, respectively. All the experiments started and ended with standard HEPES solution perfusing both sides of the cells. Experiments were performed at 37 °C. pH<sub>i</sub> was measured using a Life Sciences Microfluorimeter System (Life Sciences Resources, Cambridge, UK). About 10-15 cells were alternately excited with wavelengths of 440 and 490 nm, and the 490/440 fluorescence emission ratio was recorded at 535 nm over a sampling period of 256 ms. The resting pH<sub>i</sub> of CFPAC-1 cells in standard HEPES solution was determined using the method described by Hegyi *et al.*<sup>[21]</sup>. Calibration of 490/440 ratio to pH<sub>i</sub> was obtained using the high-K<sup>+</sup>/nigericin method. Extracellular pH was stepped between 5.94 and 8.46.

### Determination of buffering capacity

The intrinsic buffering capacity (β<sub>i</sub>) of CFPAC-1 cells was estimated according to the NH<sub>4</sub><sup>+</sup> prepulse technique<sup>[22]</sup>. Briefly, the cells were exposed to varying concentrations of NH<sub>4</sub>Cl (0-30 mmol/L) while Na<sup>+</sup> and HCO<sub>3</sub><sup>-</sup> were omitted

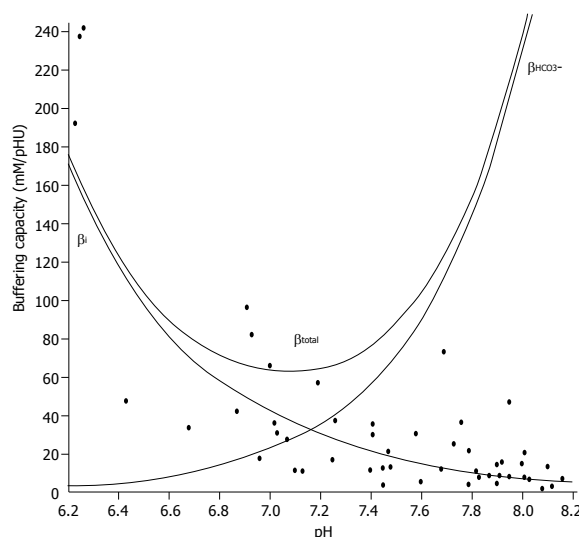


**Figure 1** Buffering capacity of CFPAC-1 human pancreatic duct cells at different pH<sub>i</sub> values. Polarized CFPAC-1 cells were exposed to varying concentrations of NH<sub>4</sub>Cl (0-30 mmol/L), while Na<sup>+</sup> and HCO<sub>3</sub><sup>-</sup> were omitted from the bath solution to block the Na<sup>+</sup> and HCO<sub>3</sub><sup>-</sup>-dependent pH regulatory mechanisms. β<sub>i</sub> was estimated by the Henderson-Hasselbalch equation (n=50). The total buffering capacity (β<sub>total</sub>) was calculated as β<sub>total</sub>=β<sub>i</sub>+β<sub>HCO<sub>3</sub><sup>-</sup></sub>, where β<sub>HCO<sub>3</sub><sup>-</sup></sub> is the buffering capacity of the HCO<sub>3</sub><sup>-</sup>/CO<sub>2</sub> system. β<sub>HCO<sub>3</sub><sup>-</sup></sub>=2.3×[HCO<sub>3</sub><sup>-</sup>]<sub>i</sub>. [HCO<sub>3</sub><sup>-</sup>]<sub>i</sub> is the intracellular concentration of HCO<sub>3</sub><sup>-</sup>.

from the bath solution to block the Na<sup>+</sup>- and HCO<sub>3</sub><sup>-</sup>-dependent pH regulatory mechanisms. β<sub>i</sub> was estimated by the Henderson-Hasselbalch equation. The total buffering capacity (β<sub>total</sub>) was calculated as β<sub>total</sub>=β<sub>i</sub>+β<sub>HCO<sub>3</sub><sup>-</sup></sub>, where β<sub>HCO<sub>3</sub><sup>-</sup></sub> is the buffering capacity of the HCO<sub>3</sub><sup>-</sup>/CO<sub>2</sub> system. β<sub>HCO<sub>3</sub><sup>-</sup></sub>=2.3×[HCO<sub>3</sub><sup>-</sup>]<sub>i</sub>. [HCO<sub>3</sub><sup>-</sup>]<sub>i</sub> is the intracellular concentration of HCO<sub>3</sub><sup>-</sup>.

### Overall ΔpH<sub>i</sub>, base flux

The overall ΔpH<sub>i</sub> was measured by determining the pH<sub>i</sub> immediately before and at the peak level during the administration of solutions containing HCO<sub>3</sub><sup>-</sup>/CO<sub>2</sub> by averaging the values of 80 data points. The initial rates of ΔpH<sub>i</sub> (over 30 s) were used to calculate transmembrane base flux J(B) using the equation J(B)=ΔpH<sub>i</sub>/Δt\*β<sub>i</sub>. The β<sub>i</sub> value used in the calculation of J(B)s was obtained from Figure 1 by using the average pH<sub>i</sub> value over a 30-s period immediately before the administration of HCO<sub>3</sub><sup>-</sup>/CO<sub>2</sub> (virtually no HCO<sub>3</sub><sup>-</sup> in the cells). Therefore, we were most likely underestimating J(B) because of the increase in buffering capacity as HCO<sub>3</sub><sup>-</sup> fluxes into the cell during the administration of the basolateral HCO<sub>3</sub><sup>-</sup>/CO<sub>2</sub> solution. The only time we used β<sub>total</sub> to calculate J(B) was when we administered basolateral standard HCO<sub>3</sub><sup>-</sup>/CO<sub>2</sub> solution during perfusion with apical standard HCO<sub>3</sub><sup>-</sup>/CO<sub>2</sub>. We denote base influx as J(B) and base efflux as -J(B).

### RT-PCR

Total RNA was extracted from CFPAC-1 cells grown in tissue culture flasks using RNAzol solution (Gibco-BRL) according to the manufacturer's instructions. For reverse transcriptase (RT)-PCR, 2 μg of RNA was reverse transcribed with 50 ng of random hexamer primers (GIBCO-BRL) in a final volume

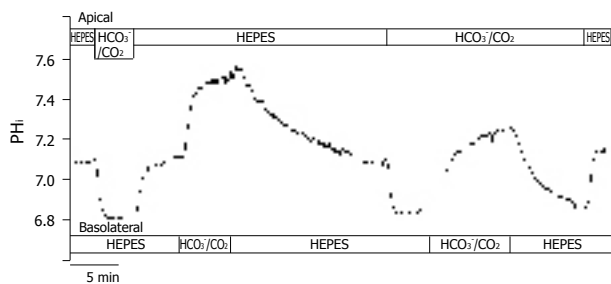


**Figure 2** Functional polarities of CFPAC-1 cells. CFPAC-1 cells were grown to confluence on permeable supports, loaded with the pH-sensitive fluorescent dye BCECF-AM (2  $\mu\text{mol/L}$ ) and mounted into a perfusion chamber, which allowed the simultaneous perfusion of different solutions to the basolateral and apical membranes. The figure shows representative  $\text{pH}_i$  traces demonstrating cell polarity. The administration of standard  $\text{HCO}_3^-/\text{CO}_2$  solution to the apical and the basolateral sides of the cells showed a marked difference in response ( $n=12-20$ ).

of 20  $\mu\text{L}$  using 50 U of Moloney murine leukemia virus RT (Fermentas) at 37  $^\circ\text{C}$  for 1 h, following the manufacturer's instructions. The primers used for PCR amplification were previously described<sup>[23-25]</sup>. NHE1: 5'-CCAGCTCATTGCCTTCTACC-3' (sense) and 5'-TGTGTCTGTTGTAGGACCGC-3' (antisense) (length of amplified region 245 residues); AE2: 5'-GAAGATTCCTGAGAATGCCG-3' (sense) and 5'-GTCCATGTTGGCACTACTCG-3' (antisense) (length of amplified region 181 residues); pancreatic NBC1 (pNBC): 5'-ATGTGTGTGATGAAGAAGAAGTAGAAG-3' (sense) and 5'-GACCGAAGGTTGGATTTCTTG-3' (antisense) (length of amplified region 621 residues); glyceraldehyde-3-phosphate dehydrogenase (GAPDH): 5'-ATGGCACCGTCAAGGCTGAGA-3' (sense) and 5'-GCATGGACTGTGGTCATGAG-3' (antisense) (length of amplified region 371 residues). The PCR reaction was started with a 3-min 94  $^\circ\text{C}$  step and was followed by standard step-cycling conditions with 30 cycles of amplification utilizing *Taq* DNA polymerase (Fermentas); the reaction was ended by a 10-min 72 $^\circ\text{C}$  step. The cycling conditions for NHE1, AE2, and GAPDH were 94  $^\circ\text{C}$  for 30 s, 58  $^\circ\text{C}$  for 30 s and 72  $^\circ\text{C}$  for 30 s; and for pNBC1 were 94  $^\circ\text{C}$  for 30 s, 58  $^\circ\text{C}$  for 30 s and 68  $^\circ\text{C}$  for 3 min. RT-PCR products were separated by electrophoresis on a 20 g/L agarose gel containing ethidium bromide (0.5  $\mu\text{g/mL}$ ) and were visualized under ultraviolet light.

### Statistical analyses

In agreement with Zsembery *et al*<sup>[26]</sup>, we noticed a variation in the rate and magnitude of  $\text{HCO}_3^-$  uptake between the different set of monolayers that we could not attribute to the passage number or time after seeding. To avoid errors arising from this fact, we (1) performed a particular experimental protocol on the same day using one set of cell cultures, (2) randomized the order in which monolayers in the same group were exposed to experimental maneuvers (i.e., exposure to inhibitors), and (3) always included internal controls where possible. Summary data in the figures are expressed as percent change from control and statistical analyses were performed using either Student's paired or unpaired *t* test or the analysis of variance as appropriate. *P* values <0.05 were considered statistically significant.

## RESULTS

### Transepithelial electrical resistance, resting $\text{pH}_i$ and buffering capacity

The CFPAC-1 cells grown on polyester Transwells became confluent in 2-3 d as judged by visual observation. The net transepithelial resistance increased steadily over 4-5 d after seeding when it reached a plateau of  $100 \pm 4 \Omega/\text{cm}^2$  ( $n=88$ ). The resting  $\text{pH}_i$  of the cells in standard HEPES solution was  $7.11 \pm 0.08$  ( $n=6$ ).

### Apical administration of $\text{HCO}_3^-/\text{CO}_2$

After perfusing both the apical and basolateral sides of the CFPAC-1 cells with standard HEPES solution, apical perfusion was switched to the standard  $\text{HCO}_3^-/\text{CO}_2$  solution (Figure 2). We then observed a rapid acidification ( $-17.5 \pm 1.5 \text{ mmol/L B/min}$ ,  $n=20$ ) of  $\text{pH}_i$ , most likely caused by the diffusion of  $\text{CO}_2$  into the cells. Following this, the  $\text{pH}_i$  reached a new approximate steady state value ( $6.82 \pm 0.02$ ,  $n=20$ ) and remained at this level until the standard HEPES solution was restored to the apical membrane. Restoration of standard HEPES solution induced a rapid alkalinization of  $\text{pH}_i$  towards the resting  $\text{pH}_i$  value probably brought about by the diffusion of  $\text{CO}_2$  from the cells. These observations suggested that  $\text{CO}_2$  influx was very fast across the apical membrane of CFPAC-1 cells, and that significant  $\text{HCO}_3^-$  influx did not occur.

### Basolateral administration of $\text{HCO}_3^-/\text{CO}_2$

After perfusion of both the apical and basolateral membranes of CFPAC-1 cells with standard HEPES solution, the basolateral perfusate was switched to standard  $\text{HCO}_3^-/\text{CO}_2$  (Figure 2). Upon changing the basolateral perfusate, there was a rapid alkalinization of  $\text{pH}_i$  ( $\Delta\text{pH}_i = 0.48 \pm 0.03$ ,  $J(\text{B}) = 15.0 \pm 2.3 \text{ mmol/L B/min}$ ,  $n=12$ ), most likely induced by the transport of  $\text{HCO}_3^-$  into the cells. Removal of the standard  $\text{HCO}_3^-/\text{CO}_2$  solution from the basolateral side induced a further small transient increase in  $\text{pH}_i$  consistent with efflux of  $\text{CO}_2$ , followed by a slow acidification towards the resting  $\text{pH}_i$  value brought about by the extrusion of  $\text{HCO}_3^-$  (Figure 2). These observations suggested that  $\text{HCO}_3^-$  might cross the basolateral membrane of CFPAC-1 cells much faster than  $\text{CO}_2$ . To rule out the possibility that basolateral  $\text{HCO}_3^-$  entry was at least partly due to  $\text{CO}_2$  influx, followed by its rapid hydration to  $\text{HCO}_3^-$  ions, we perfused the apical side of CFPAC-1 cells with a standard  $\text{HCO}_3^-/\text{CO}_2$  solution for 4 min (intracellular  $\text{pCO}_2$  was increased) and then the same solution was added to the basolateral side (Figure 2). Under these conditions we still observed a rapid alkalinization of  $\text{pH}_i$  ( $\Delta\text{pH}_i = 0.40 \pm 0.05$ ,  $J(\text{B}) = 14.1 \pm 1.9 \text{ mmol/L B/min}$ ,  $n=6$ ) which was not significantly different compared to the absence of apical  $\text{HCO}_3^-/\text{CO}_2$ .

Taken together with the effects of apical  $\text{HCO}_3^-/\text{CO}_2$  administration, these data showed that CFPAC-1 monolayers exhibited functional polarity with respect to  $\text{HCO}_3^-$  transport. Subsequently, we used the apical administration of  $\text{HCO}_3^-/\text{CO}_2$  to check the functional polarity of monolayers at the beginning of each experiment. The cells were considered to be polarized, if



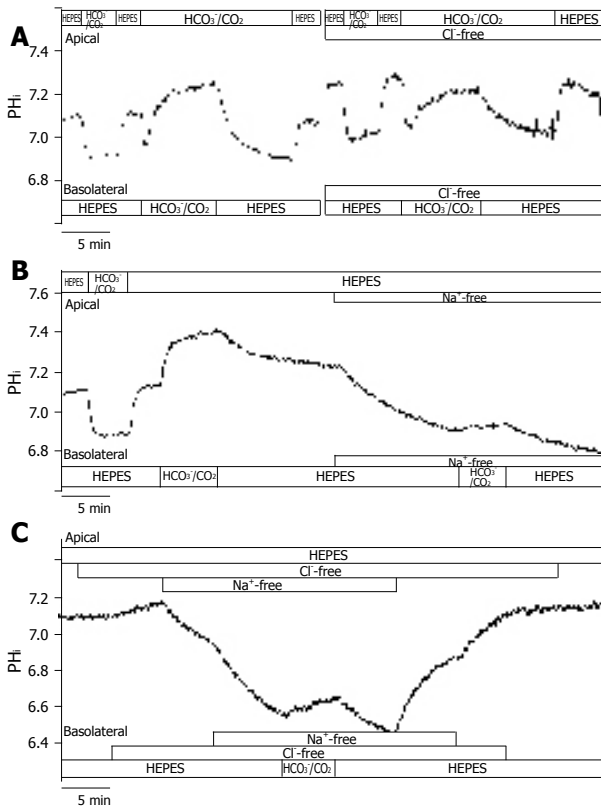


**Figure 3** Basolateral  $\text{HCO}_3^-$  uptake – effects of  $\text{Cl}^-$  and/or  $\text{Na}^+$  withdrawal. The figure shows representative  $\text{pHi}$  traces. **A:** The rate of  $\text{HCO}_3^-$  uptake was significantly decreased in  $\text{Cl}^-$ -free conditions compared to standard conditions ( $J(B) = 73.1 \pm 7.2\%$  and  $100 \pm 8.5\%$ , respectively,  $n = 5$ ); **B:** The administration of basolateral  $\text{HCO}_3^-/\text{CO}_2$  in  $\text{Na}^+$ -free conditions ( $n = 6$ ) greatly decreased  $\Delta\text{pHi}$  and  $J(B)$  compared to standard conditions, suggesting that a large proportion of the  $\text{HCO}_3^-$  uptake was due to a  $\text{Na}^+$ -sensitive process, most likely NBC; **C:** Interestingly, the decrease in the rate of  $\text{HCO}_3^-$  uptake was obviously ameliorated in the absence of both  $\text{Na}^+$  and  $\text{Cl}^-$  ( $n = 6$ ) compared to the  $\text{Na}^+$ -free condition.

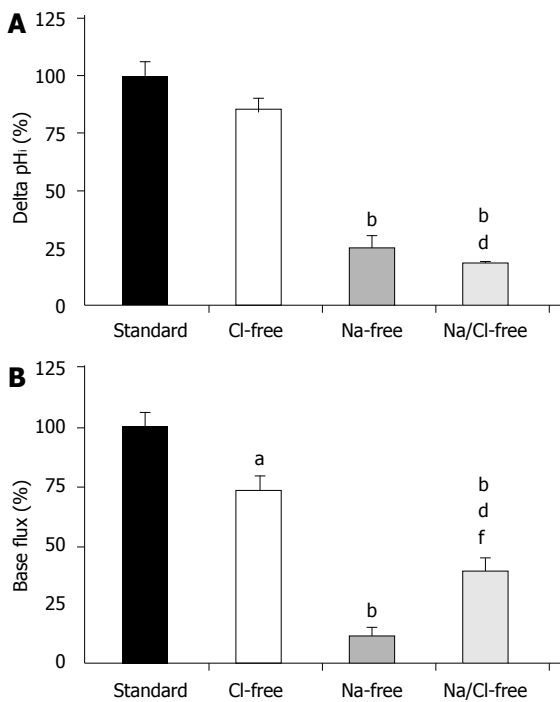


**Figure 4** Basolateral  $\text{HCO}_3^-$  uptake – changes in (A)  $\Delta\text{pHi}$  and (B)  $J(B)$  caused by the withdrawal of  $\text{Cl}^-$  and/or  $\text{Na}^+$ . SE of the control groups (standard, black bar) is somewhat different for each of the respective ion-withdrawal groups. The SEs depicted on the standard bars are the maximum values observed. <sup>a</sup> $P < 0.05$  and <sup>b</sup> $P < 0.01$  vs control group <sup>c</sup> $P < 0.01$  vs  $\text{Cl}^-$ -free group and/or <sup>d</sup> $P < 0.01$  vs  $\text{Na}^+$ -free group.

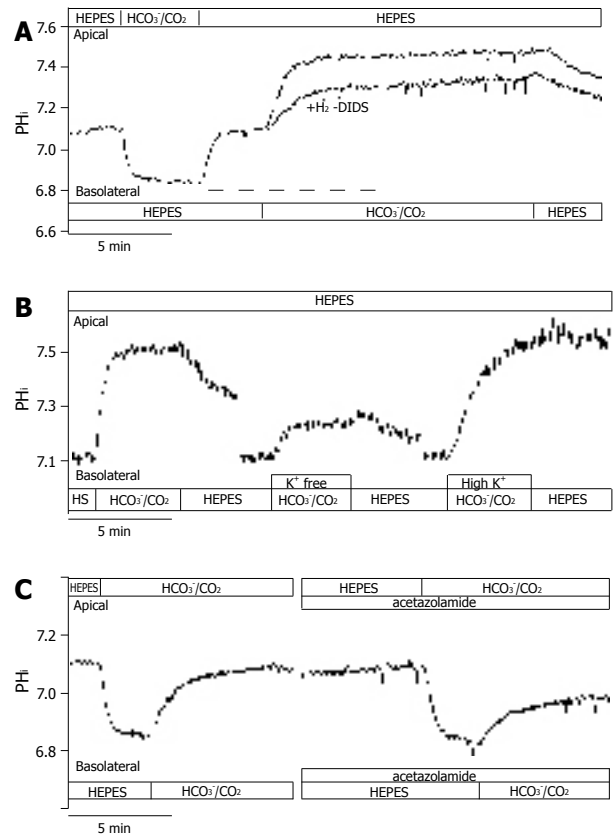


**Figure 5** Basolateral  $\text{HCO}_3^-$  uptake – effects of  $\text{H}_2\text{-DIDS}$ , acetazolamide and varying extracellular  $\text{K}^+$  concentration. The figure shows representative  $\text{pHi}$  traces. **A:** The anion transport inhibitor  $600 \mu\text{mol/L}$   $\text{H}_2\text{-DIDS}$  (added to the basolateral membrane of cells for 2 min before and during the administration of basolateral  $\text{HCO}_3^-/\text{CO}_2$ ; dashed line,  $n = 6$ ) significantly decreased the extent of alkalization ( $\Delta\text{pHi}$ ) and rate of  $J(B)$  ( $n = 6$ ); **B:** Varying extracellular  $[\text{K}^+]$  caused significant differences in  $\Delta\text{pHi}$  and  $J(B)$  ( $n = 9-11$ ); **C:** The application of the membrane-permeable carbonic anhydrase inhibitor acetazolamide ( $100 \mu\text{mol/L}$ ,  $n = 6$ ) significantly decreased the overall  $\Delta\text{pHi}$  and  $J(B)$ . HS: HEPES.

the  $\text{pHi}$  remained constant after the initial decrease in  $\text{pHi}$  caused by the diffusion of  $\text{CO}_2$  into the cells.

**Investigation of basolateral  $\text{HCO}_3^-$  uptake**

In theory, the alkalization observed after the administration of basolateral standard  $\text{HCO}_3^-/\text{CO}_2$  could be explained by the action of the NBC and the reversal of  $\text{Cl}^-/\text{HCO}_3^-$  anion exchanger. The initial rate of  $\text{HCO}_3^-$  uptake was significantly decreased in  $\text{Cl}^-$ -free vs standard conditions ( $J(B) = 73.1 \pm 7.2\%$  and  $100 \pm 8.5\%$ , respectively,  $n = 5$ , Figures 3A and 4); however, no significant difference was noted for the overall  $\Delta\text{pHi}$  for the two groups ( $85.5 \pm 6.0\%$  and  $100 \pm 6.3\%$ , respectively). The administration of basolateral  $\text{HCO}_3^-/\text{CO}_2$  greatly decreased  $\Delta\text{pHi}$  ( $25.6 \pm 5.1\%$ ) and  $J(B)$  ( $11.7 \pm 2.3\%$ ) in  $\text{Na}^+$ -free conditions ( $n = 6$ ) compared to those ( $100 \pm 7.5\%$  and,  $100 \pm 10.7\%$ , respectively) in standard conditions, suggesting that a large proportion of the  $\text{HCO}_3^-$  uptake was due to a  $\text{Na}^+$ -sensitive process, most likely via an NBC (Figures 3B and 4). Interestingly, the decrease in the rate of  $\text{HCO}_3^-$  uptake was somewhat attenuated in the absence of both  $\text{Na}^+$  and  $\text{Cl}^-$  [ $n = 6$ ,  $J(B)$  changed to  $38.4 \pm 6.9\%$ , Figures 3C and 4].

To further confirm the presence of NBC on the basolateral membrane of CFPAC-1 cells, we examined the recovery from a  $\text{Na}^+$ -free acid load in the presence

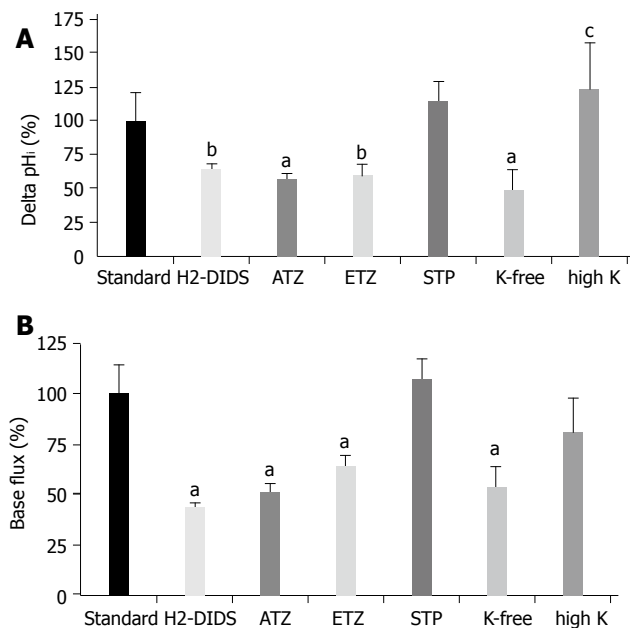


**Figure 6** Basolateral  $\text{HCO}_3^-$  uptake – changes in (A)  $\Delta\text{pH}_i$  (B)  $J(\text{B})$  caused by application of  $\text{H}_2\text{-DIDS}$ , acetazolamide, ethoxzolamide, STP and varying extracellular  $\text{K}^+$  concentration. Data are shown as mean  $\pm$  SE ( $n=6-11$ ). SE of the control groups (standard, black bar) is somewhat different for each of the respective ion-withdrawal groups. The SE depicted on the control bar was the maximum values observed. <sup>a</sup> $P<0.05$  and <sup>b</sup> $P<0.01$  vs control group or <sup>c</sup> $P<0.05$  vs  $\text{K}^+$ -free group. ATZ: acetazolamide; ETZ: ethoxzolamide; STP: 1-*N*-(4-sulfamoylphenylethyl)-2,4,6-trimethylpyridine perchlorate. The SE depicted on the standard bars was the maximum values observed.

of  $\text{HCO}_3^-/\text{CO}_2$  by adding basolateral  $\text{Na}^+$  with/without 300  $\mu\text{mol/L}$  amiloride (to block basolateral  $\text{Na}^+/\text{H}^+$  exchange,  $n=6$ ). After acid loading of cells, the basolateral addition of  $\text{Na}^+$  stimulated a  $J(\text{B})$  of  $39.0\pm 4.4$  mmol/L B/min (please see below the much lower values in HEPES solution). In contrast, the basolateral addition of  $\text{Na}^+$  in the presence of amiloride decreased this value to  $22.2\pm 3.6$  mmol/L B/min, suggesting that a third pathway of acid transport is due to a basolateral NHE. The anion transport inhibitor  $\text{H}_2\text{-DIDS}$  (600  $\mu\text{mol/L}$ , added to the basolateral membrane of cells for 2 min before and during the administration of basolateral  $\text{HCO}_3^-/\text{CO}_2$ ,  $n=6$ ), significantly decreased the extent of alkalization ( $\Delta\text{pH}_i$ ) to  $63.2\pm 4.7\%$  and rates of  $J(\text{B})$  to  $43.9\pm 5.1\%$  ( $n=6$ , Figures 5A and 6). Varying the extracellular  $\text{K}^+$  concentrations ( $\text{K}^+$ -free, high  $\text{K}^+$ ,  $n=9-11$ ) of the basolateral standard  $\text{HCO}_3^-/\text{CO}_2$  solution induced significant differences between the  $\Delta\text{pH}_i$  values vs the standard  $\text{HCO}_3^-/\text{CO}_2$  solution ( $41.5\pm 24.5\%$ ,  $139.6\pm 15.0\%$  and  $100\pm 11.1\%$ , respectively; Figures 5B and 6). The  $J(\text{B})$  significantly decreased when  $\text{K}^+$ -free  $\text{HCO}_3^-/\text{CO}_2$  ( $73.9\pm 6.4\%$ ) was administered to the basolateral membrane, but was not affected by high  $\text{K}^+$ ,  $\text{HCO}_3^-/\text{CO}_2$  ( $96.6\pm 11.0\%$ ) vs the standard  $\text{HCO}_3^-/\text{CO}_2$  solution ( $100.0\pm 15.8\%$ ). Thus, our experiments showed that alteration of the membrane potential of CFPAC-1 cells, by varying basolateral extracellular  $\text{K}^+$  concentration, modified the extent of  $\text{HCO}_3^-$  uptake. The application of the membrane permeable CA inhibitors acetazolamide (100  $\mu\text{mol/L}$ ,  $n=6$ , Figures 5C and 6) or ethoxzolamide (100  $\mu\text{mol/L}$ ,

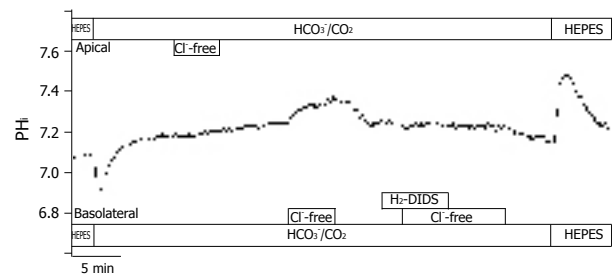


**Figure 7** Localization of  $\text{Cl}^-/\text{HCO}_3^-$  exchangers in CFPAC-1 cells. The figure shows representative  $\text{pH}_i$  traces ( $n=6$ ). The localization of  $\text{Cl}^-/\text{HCO}_3^-$  exchangers was performed by measuring the effect of changes in  $\text{Cl}^-$  gradient across the luminal or basolateral membranes on  $\text{pH}_i$ . In the presence of  $\text{HCO}_3^-$ , the removal of  $\text{Cl}^-$  from the apical membrane did not result in changes of  $\text{pH}_i$ . The removal of  $\text{Cl}^-$  from the basolateral membrane caused a  $\Delta\text{pH}_i$  of  $0.08\pm 0.01$  and a  $J(\text{B})$  of  $4.37\pm 0.46$  mmol/L B/min. Furthermore, the basolateral administration of 250  $\mu\text{mol/L}$   $\text{H}_2\text{-DIDS}$  completely blocked  $\text{pH}_i$  changes caused by the withdrawal of  $\text{Cl}^-$ .

$n=6$ ) in the apical (standard  $\text{HCO}_3^-/\text{CO}_2$  solution) and basolateral (standard HEPES solution) perfusions, 10 min before and during the administration of basolateral standard  $\text{HCO}_3^-/\text{CO}_2$  solution, significantly decreased the overall  $\Delta\text{pH}_i$  to  $56.8\pm 4.2\%$  or  $59.0\pm 9.8\%$ , and  $J(\text{B})$  to  $50.5\pm 4.6\%$  or  $63.7\pm 8.3\%$ , respectively. The basolateral addition of the membrane impermeable CA inhibitor STP (10  $\mu\text{mol/L}$ ,  $n=6$ ) in standard HEPES solution (the apical side of the cells was perfused with standard  $\text{HCO}_3^-/\text{CO}_2$  solution), 5 min before and during the administration of basolateral standard  $\text{HCO}_3^-/\text{CO}_2$  solution, did not significantly influence overall  $\Delta\text{pH}_i$  ( $114.3\pm 14.3\%$ ) and  $J(\text{B})$  ( $106.7\pm 17.9\%$ , Figure 6).

#### Localization of $\text{Cl}^-/\text{HCO}_3^-$ exchangers in CFPAC-1 cells

The localization of  $\text{Cl}^-/\text{HCO}_3^-$  exchangers was performed by measuring the effect of changes in  $\text{Cl}^-$  gradient across the luminal and/or basolateral membranes on  $\text{pH}_i$ . In the presence of  $\text{HCO}_3^-$ , the removal of  $\text{Cl}^-$  from the apical membrane did not result in changes of  $\text{pH}_i$ . The removal of  $\text{Cl}^-$  from the basolateral membrane caused a  $\Delta\text{pH}_i$  of  $0.08\pm 0.01$  and a  $J(\text{B})$  of  $4.4\pm 0.5$  mmol/L B/min ( $n=6$ , Figure 7). Furthermore, the basolateral administration of 250  $\mu\text{mol/L}$   $\text{H}_2\text{-DIDS}$  (from 2 min before changing the solution to  $\text{Cl}^-$ -free  $\text{HCO}_3^-/\text{CO}_2$ ) completely blocked  $\text{pH}_i$  changes caused by the withdrawal of  $\text{Cl}^-$ . However, 10  $\mu\text{mol/L}$  forskolin, 100  $\mu\text{mol/L}$  acetazolamide or 100  $\mu\text{mol/L}$  ethoxzolamide (from 10 min before changing the solution to  $\text{Cl}^-$ -free  $\text{HCO}_3^-/\text{CO}_2$ ) did not significantly influence  $\text{Cl}^-/\text{HCO}_3^-$  exchange on the apical and basolateral membranes ( $n=6-8$ , data not shown).

#### Localization of $\text{Na}^+/\text{H}^+$ exchangers in CFPAC-1 cells

In HEPES-buffered solutions, the removal of  $\text{Na}^+$  from the perfusing solutions had a small acidifying effect on  $\text{pH}_i$  [ $J(\text{B})=1.00\pm 0.13$  mmol/L B/min,  $n=12$ ]. After exposure and then removal of the  $\text{NH}_4^+$  in the absence of  $\text{Na}^+$  on both sides of the duct cells,  $\text{pH}_i$  reduced to  $6.73\pm 0.03$  ( $n=12$ ), and stabilized at this level (Figure 8A). We could not detect any active  $\text{H}^+$ -pumps in CFPAC-1 cells, since  $\text{pH}_i$  did not increase in the absence of extracellular  $\text{Na}^+$ . Re-addition of  $\text{Na}^+$  to the apical or the basolateral side caused  $\text{pH}_i$  recovery towards the resting values [ $J(\text{B})=-6.6$

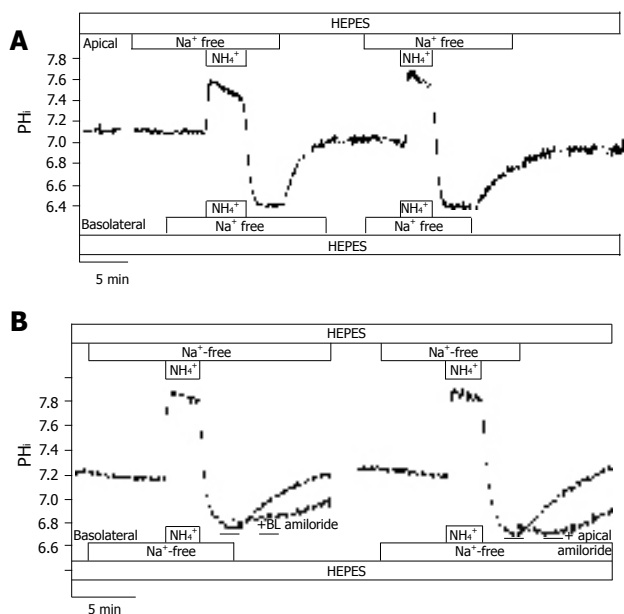


**Figure 8** Localization of  $\text{Na}^+/\text{H}^+$  exchangers in CFPAC-1 cells. The figure shows representative  $\text{pH}_i$  traces. **A:** After exposure to  $\text{NH}_4^+$  in the absence of  $\text{Na}^+$  on both sides of the duct cells,  $\text{pH}_i$  reduced to  $6.73 \pm 0.03$  ( $n=12$ ), and stabilized at this level. We could not detect any active  $\text{H}^+$ -pumps in CFPAC-1 cells, since  $\text{pH}_i$  did not increase in the absence of extracellular  $\text{Na}^+$ . Upon addition of  $\text{Na}^+$  to the apical or the basolateral side prompted the  $\text{pH}_i$  to recover towards the resting values ( $n=6-10$ ); **B:** The administration of 300  $\mu\text{mol/L}$  amiloride (dashed line) to the  $\text{Na}^+$ -free (from 2 min before the addition of  $\text{Na}^+$ ) and  $\text{Na}^+$ -containing HEPES solutions prevented the recovery of  $\text{pH}_i$  in the presence of  $\text{Na}^+$  ( $n=6$ ). Removal of amiloride resulted in the recovery of  $\text{pH}_i$  to resting values.

$\pm 2.6$  mmol/L B/min and  $-7.5 \pm 1.3$  mmol/L B/min, respectively,  $n=6-10$ ]. The administration of 300  $\mu\text{mol/L}$  amiloride to the  $\text{Na}^+$ -free (from 2 min before the addition of  $\text{Na}^+$ ) and  $\text{Na}^+$ -containing HEPES solutions prevented the recovery of  $\text{pH}_i$  in the presence of  $\text{Na}^+$  ( $n=6$ , Figure 8B). Removing amiloride resulted in the recovery of  $\text{pH}_i$  to resting values. Interestingly, the removal of apical  $\text{Na}^+$  from the standard  $\text{HCO}_3^-/\text{CO}_2$  solution perfusing CFPAC-1 cells caused a sudden but small acidification of  $\text{pH}_i$  ( $\Delta\text{pH}_i = 0.14 \pm 0.01$  and  $J(\text{B}) = -10.8 \pm 0.8$  mmol/L B/min,  $n=6$ ), whereas we did not see any change in  $\text{pH}_i$  when we removed  $\text{Na}^+$  from the basolateral side of the cells ( $n=6$ ). Taken together, our experiments showed that there are  $\text{Na}^+/\text{H}^+$  exchangers on both the apical and the basolateral membranes. Finding a  $\text{Na}^+/\text{H}^+$  exchanger on the apical side was somewhat unexpected. A possible explanation for this would be that the cells were leaky to  $\text{Na}^+$  ions. However, despite the great difference in  $\text{Na}^+$  concentration (0 mmol/L *vs* 140 mmol/L) of the apical and basolateral perfusates, analysis of the  $\text{Na}^+$  concentration of the solutions by mass spectrometry showed no contamination during perfusion.

#### Molecular identification of $\text{H}^+$ and $\text{HCO}_3^-$ transporters

To further investigate the presence of different  $\text{H}^+$  and  $\text{HCO}_3^-$  transporters in CFPAC-1 cells, we undertook RT-PCR analysis. We could detect mRNA expressions for pNBC1, AE2, and NHE1; the housekeeping gene GAPDH was used to normalize mRNA levels (Figure 9).

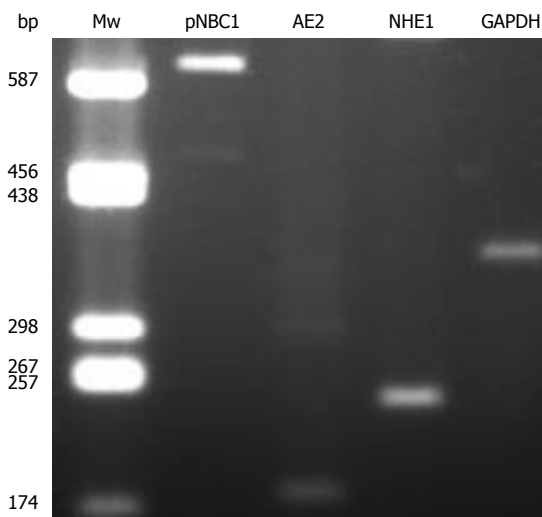


**Figure 9** Expression of pNBC1, AE2, NHE1, and GAPDH mRNA in CFPAC-1 cells. Mw: molecular weight ladder (bp indicates number of base pairs).

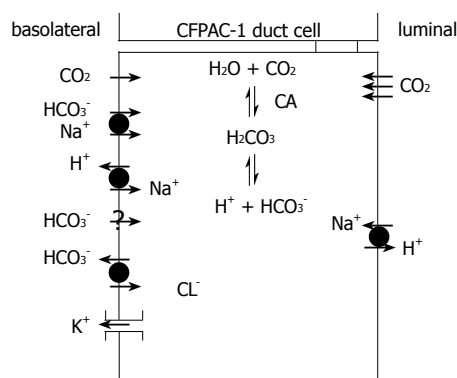


**Figure 10**  $\text{H}^+$  and  $\text{HCO}_3^-$  transport mechanisms in CFPAC-1 human pancreatic duct cells. The basolateral membrane expresses  $\text{Na}^+/\text{HCO}_3^-$  co-transporters,  $\text{Na}^+/\text{H}^+$  exchangers and  $\text{Cl}^-/\text{HCO}_3^-$  exchangers plus an unidentified  $\text{Na}^+$ -independent  $\text{HCO}_3^-$  entry pathway. These transporters facilitate the rapid flux of  $\text{HCO}_3^-$  ions into the cell.  $\text{K}^+$  channels are also likely to be expressed on the basolateral membrane because altering extracellular  $\text{K}^+$  concentration affects  $\text{HCO}_3^-$  influx. The apical membrane expresses  $\text{Na}^+/\text{H}^+$  exchangers, but not CFTR and  $\text{Cl}^-/\text{HCO}_3^-$  exchangers found in normal pancreatic duct cells. The apical membrane is an effective barrier to  $\text{HCO}_3^-$  influx from the lumen, but is freely permeable to  $\text{CO}_2$ . CA: Carbonic anhydrase.

## DISCUSSION

Our results showed the functional presence of the NBC and  $\text{Cl}^-/\text{HCO}_3^-$  exchanger on the basolateral membrane, together with  $\text{Na}^+/\text{H}^+$  exchangers on both the apical and basolateral membranes of CFPAC-1 cells (Figure 10). That there was no detectable  $\text{Cl}^-/\text{HCO}_3^-$  exchange activity on the apical membrane was not a surprise as CFTR is known to be required for its activation<sup>[3,27]</sup>. RT-PCR revealed the expression of pNBC1, AE2, and NHE1 mRNA.

CFPAC-1 cells clearly demonstrated a differential permeability to  $\text{HCO}_3^-$  at the apical and basolateral membranes. We found that the addition of 25 mmol/L  $\text{HCO}_3^-/\text{CO}_2$  to the basolateral side of the cells caused a marked alkalization of  $\text{pH}_i$ , whereas exposing the apical membrane to the same solution caused a sustained acidification. These data suggest that the basolateral membrane of CFPAC-1 cells is much more permeable

to  $\text{HCO}_3^-$  than the apical membrane. Plasma membrane  $\text{HCO}_3^-$  and  $\text{CO}_2$  permeabilities have been reported to vary in different species and tissues. In perfused rabbit gastric glands, the luminal membranes of parietal and chief cells were impermeable to  $\text{HCO}_3^-$  and  $\text{CO}_2$ , while the basolateral membranes were permeable to both<sup>[28]</sup>. Apical  $\text{HCO}_3^-$  permeability is relatively low in cultured bovine corneal endothelial cells<sup>[29]</sup>. In contrast,  $\text{HCO}_3^-$  permeability of the apical side of intact colonic mucosa of guinea pig is markedly higher<sup>[30]</sup>. Our results are in accordance with similar observations made by Ishiguro *et al.*<sup>[31]</sup> using guinea pig ducts. Administration of 25 mmol/L  $\text{HCO}_3^-/\text{CO}_2$  to the lumen of microperfused guinea pig pancreatic ducts decreased  $\text{pH}_i$  rapidly. Following this, no subsequent increase in  $\text{pH}_i$  was observed, indicating that little  $\text{HCO}_3^-$  was able to enter the cell from the lumen.  $\text{HCO}_3^-$  entry was detected only when the luminal  $\text{HCO}_3^-$  concentration was raised above 125 mmol/L. A low apical  $\text{HCO}_3^-$  permeability would make physiological sense in species, such as man and guinea pig, which can secrete near isotonic  $\text{NaHCO}_3$ . Our work is the first demonstration of  $\text{HCO}_3^-/\text{CO}_2$  asymmetry in polarized human pancreatic duct cells. Finally, it seems that CFPAC-1 cells, which express  $\Delta\text{F508 CFTR}$ , exhibit the same resistance to  $\text{HCO}_3^-$  influx across the apical membrane as native guinea pig duct cells. This suggests that the presence of functional CFTR in the apical membrane is not required for this membrane to act as an effective barrier to  $\text{HCO}_3^-$  influx from the lumen.

A large proportion of the basolateral  $\text{HCO}_3^-$  uptake was  $\text{Na}^+$ -dependent and was partially inhibited by  $\text{H}_2\text{-DIDS}$ , therefore, it is most likely due to the action of  $\text{pNBC1}$ . However, we also detected a novel  $\text{Na}^+$ -independent  $\text{HCO}_3^-$  influx mechanism that was significantly increased in  $\text{Cl}^-$ -free conditions, the identity of which remains unknown. NBCs have been detected in the guinea pig<sup>[32,33]</sup>, rat<sup>[34,35]</sup> and mouse<sup>[36]</sup>. In contrast, Novak *et al.*<sup>[37,38]</sup> could not detect any  $\text{HCO}_3^-$  uptake by NBC in freshly prepared rat pancreatic ducts using electrophysiological and  $\text{pH}_i$  measurements. Extracellular  $\text{HCO}_3^-/\text{CO}_2$  did not increase the rate of  $\text{pH}_i$  recovery in experimental acidosis. The expressions of NBC mRNA and protein have been noted in the human pancreas<sup>[39]</sup>. Immunofluorescence localized the transporter to the basolateral but not the apical membrane of the pancreatic duct cells. Interestingly, immunohistological studies have shown the NBC in both the apical and basolateral membranes of rat pancreatic duct cells<sup>[35]</sup>. NBC1 mRNA was also detected in CFPAC-1 cells by Northern hybridization<sup>[13]</sup>. In accordance with our findings, expression of NBC1 was also found in non-polarized cells by recovery from acidosis in the presence of  $\text{HCO}_3^-$ ,  $\text{Na}^+$  and amiloride and its sensitivity to the administration of 200  $\mu\text{mol/L}$  DIDS<sup>[13]</sup>. cAMP had no effect on NBC activity in CFPAC-1 cells, whereas NBC activity was stimulated in CAPAN-1 cells expressing wild-type CFTR<sup>[13]</sup>. The basolateral localization of the NBC was shown by  $^{22}\text{Na}^+$  flux studies in CFPAC-1 cells stably transfected with wild-type CFTR grown on permeable supports (no data was reported for untransfected CFPAC-1 cells)<sup>[13]</sup>.

The application of the membrane permeable CA

inhibitor acetazolamide or ethoxzolamide partially inhibited the rate of basolateral base flux in CFPAC-1 cells, whereas the membrane-impermeable CA inhibitor STP<sup>[40]</sup> had no such effect. Carbonic anhydrases are known to be coupled to  $\text{HCO}_3^-$  transporters, such as  $\text{Cl}^-/\text{HCO}_3^-$  anion exchangers<sup>[41-44]</sup>,  $\text{DRA}$ <sup>[45]</sup> and  $\text{NBC}$ <sup>[46]</sup>. There are at least 14 different isoenzymes in the  $\alpha$ -CA gene family present in vertebrates<sup>[47]</sup>. CA I-III and VII are cytosolic, while CA IV, IX, XII and XIII are membrane-associated, V is mitochondrial and VI is secreted. Of the 14 different isoforms, CA II, IV, IX and XII were shown to be expressed in the human pancreas and cultured pancreatic tumor cells<sup>[48]</sup>. Interestingly, CA II and IV expressions were found to be associated with apical  $\text{HCO}_3^-$  channels in human pancreatic duct cells CAPAN-1<sup>[49]</sup>, although the targeting of CA IV to the apical plasma membrane was impaired in the CFPAC-1 cells<sup>[50]</sup>. Kivela *et al.*<sup>[51]</sup> have clearly detected the transmembrane CA isoenzymes IX and XII on the basolateral membrane of the normal and pathological pancreas by immunohistochemistry. However, it is unlikely that the latter isoenzymes are associated with NBC as STP had no inhibitory effect on  $\text{HCO}_3^-$  uptake. Furthermore, in accordance with our results, Cheng *et al.*<sup>[52]</sup> have shown in CAPAN-1 cells that  $\text{HCO}_3^-$ -dependent forskolin-induced  $I_{sc}$  could be significantly reduced by acetazolamide. Moreover, the CA inhibitor also had an inhibitory effect on dome formation, which was thought to be due to exchange of water and electrolytes<sup>[49]</sup>. Taken together, intracellular CAs may be involved in the rapid basolateral transport of  $\text{HCO}_3^-$  by NBC. The enzyme converts  $\text{HCO}_3^-$  to carbonic acid and possibly maintains a concentration gradient for  $\text{HCO}_3^-$  across the basolateral membrane of CFPAC-1 cells.

Alteration of extracellular  $\text{K}^+$  concentration significantly influenced  $\text{HCO}_3^-$  uptake in our experiments. The presence of  $\text{K}^+$  channels in the basolateral membranes of CFPAC-1 cells is highly likely, and one report has identified ATP-sensitive  $\text{K}^+$  channels<sup>[53]</sup> in these cells. A basolateral  $\text{K}^+$  conductance will influence the rate of  $\text{HCO}_3^-$  secretion by altering the cells membrane potential. In our experiments, high extracellular  $\text{K}^+$  concentrations increased  $\text{HCO}_3^-$  entry, which was likely due to basolateral membrane depolarization, and a consequent increase in the electrochemical driving force for  $\text{HCO}_3^-$  entry on the electrogenic NBC. In contrast, low extracellular  $\text{K}^+$  concentration inhibited  $\text{HCO}_3^-$  uptake, probably due to membrane hyperpolarization.

Novak and Greger<sup>[37]</sup> demonstrated that the basolateral membrane of rat intra- and inter-lobular pancreatic ducts had a relatively large  $\text{K}^+$  conductance, which could be decreased by the  $\text{K}^+$  channel blocker  $\text{Ba}^{2+}$ . The luminal membrane had no significant  $\text{K}^+$  conductance. Interestingly, Fong *et al.*<sup>[54]</sup> detected  $\text{K}^+$  conductances not only on the basolateral but also on the apical sides of HPAF human pancreatic duct cells.

CFPAC-1 cells exhibited  $\text{Na}^+/\text{H}^+$  exchange activity on both the apical and basolateral membranes (the latter is most likely to be due to NHE1).  $\text{Na}^+/\text{H}^+$  exchangers were identified in guinea pig<sup>[10,28-30]</sup>, rat<sup>[55,56]</sup> and mouse<sup>[8]</sup> pancreatic ducts. These exchangers were localized to the basolateral membrane of intra/interlobular duct cells.



However, the main and common segments of the rat pancreatic ducts also showed  $\text{Na}^+/\text{H}^+$  exchange activity in the apical membrane<sup>[10]</sup>. There is also evidence for an apical  $\text{Na}^+/\text{H}^+$  exchanger in bovine main pancreatic duct segments<sup>[57]</sup>. Furthermore, the main pancreatic duct of mice expressed NHE1 in the basolateral membrane, and NHE2 and NHE3 in the luminal membrane<sup>[8]</sup>. Disruption of the NHE2 gene had no effect on luminal  $\text{H}^+$  transport, while disruption of the NHE3 gene reduced luminal  $\text{Na}^+$ -dependent  $\text{H}^+$  efflux by 45%. The remaining 55% of the luminal  $\text{Na}^+$ -dependent  $\text{H}^+$  efflux from NHE3-knockout mice was inhibited by 50  $\mu\text{mol/L}$  HOE694.  $\text{Na}^+$ -dependent  $\text{H}^+$  transport mechanisms were inhibited by cAMP, therefore, they are thought to be inhibited during stimulated secretion and are most likely to be active during the resting state<sup>[8]</sup>. CFTR in the pancreatic duct not only affected the activity, but also the expression of NHE3 protein<sup>[7]</sup>. NHE3 expression was reduced by about 50%, luminal  $\text{Na}^+$ -dependent and HOE694-sensitive recovery from acid load was reduced by 60% in the ducts of  $\Delta 508$  CFTR mice<sup>[7]</sup>. To our knowledge, we are the first to detect NHEs on both the apical and basolateral membranes of human pancreatic duct cells. The presence of NHE on the apical membrane was unexpected, since it acted against  $\text{HCO}_3^-$  secretion. We do not know which section of the pancreatic duct CFPAC-1 cells originate from, but they might be from the main region where the expression of the apical NHEs was noted in animal studies. In accordance with our results, failure of  $\text{pHi}$  to recover from acid loading in the absence of extracellular  $\text{Na}^+$  suggests that there is little  $\text{H}^+$ -pump activity in the unstimulated guinea pig ducts<sup>[32]</sup>. This is in contrast with the observations made in rat<sup>[10]</sup> and pig<sup>[58]</sup> pancreatic ducts, which showed  $\text{H}^+$ -pump activity.

The role of apical  $\text{Cl}^-/\text{HCO}_3^-$  exchangers in pancreatic ductal  $\text{HCO}_3^-$  secretion is a controversial issue. One hypothesis is that all of the  $\text{HCO}_3^-$  is secreted on an anion exchanger and that CFTR's role is to activate the exchangers and to provide a route for the recycling of  $\text{Cl}^-$  across the apical membrane<sup>[59]</sup>. An alternative proposal is that  $\text{HCO}_3^-$  secretion occurs on the exchanger until the luminal concentration reaches about 70  $\text{mmol/L}$  after which  $\text{HCO}_3^-$  exits the duct cell via CFTR<sup>[60]</sup>. Previously, it has been shown that CFPAC-1 cells express AE2 on their basolateral membrane (which was also confirmed in our study) and SLC26A3 (DRA) and SLC26A6 (PAT1) on their apical membrane, and that expression of the apical SLC26 exchangers is upregulated by CFTR<sup>[14]</sup>. In accordance with these data, we observed basolateral  $\text{Cl}^-/\text{HCO}_3^-$  exchange activity (which was inhibited by  $\text{H}_2\text{-DIDS}$ ) in wild-type CFPAC-1 cells, but no apical activity, presumably due to the lack of CFTR. We also found that forskolin had no effect on either the basolateral or apical anion exchange in CFPAC-1 cells.

In conclusion, apart from the lack of CFTR and apical  $\text{Cl}^-/\text{HCO}_3^-$  exchange activity, CFPAC-1 cells have similar  $\text{H}^+$  and  $\text{HCO}_3^-$  transporters to those observed in native animal tissue. Moreover, intracellular CAs appear to play a role in the basolateral uptake of  $\text{HCO}_3^-$ . Taken together, polarized CFPAC-1 human pancreatic duct cells are likely to be a useful model to study  $\text{H}^+$  and  $\text{HCO}_3^-$  transporters,

and their dependence on CFTR, in human pancreatic duct cells.

## ACKNOWLEDGMENTS

We thank Professor RA Frizzell for kindly providing us with the CFPAC-1 cells, and Professor C Supuran for providing the 1-N-(4-sulfamoylphenylethyl)-2,4,6-trimethylpyridine perchlorate.

## REFERENCES

- 1 **Steward MC**, Ishiguro H, Case RM. Mechanisms of bicarbonate secretion in the pancreatic duct. *Annu Rev Physiol* 2005; **67**: 377-409
- 2 **Argent BE**, Gray MA, Steward MC, Case RM. Cell physiology of pancreatic ducts. In: Johnson LR eds *Physiology of the Gastrointestinal Tract*, 4th edn. Elsevier, San Diego, 2005 (in press)
- 3 **Ko SB**, Shcheynikov N, Choi JY, Luo X, Ishibashi K, Thomas PJ, Kim JY, Kim KH, Lee MG, Naruse S, Muallem S. A molecular mechanism for aberrant CFTR-dependent  $\text{HCO}_3^-$  transport in cystic fibrosis. *EMBO J* 2002; **21**: 5662-5672
- 4 **Gray MA**, Pollard CE, Harris A, Coleman L, Greenwell JR, Argent BE. Anion selectivity and block of the small-conductance chloride channel on pancreatic duct cells. *Am J Physiol* 1990; **259**: C752-C761
- 5 **Linsdell P**, Tabcharani JA, Rommens JM, Hou YX, Chang XB, Tsui LC, Riordan JR, Hanrahan JW. Permeability of wild-type and mutant cystic fibrosis transmembrane conductance regulator chloride channels to polyatomic anions. *J Gen Physiol* 1997; **110**: 355-364
- 6 **Choi JY**, Muallem D, Kiselyov K, Lee MG, Thomas PJ, Muallem S. Aberrant CFTR-dependent  $\text{HCO}_3^-$  transport in mutations associated with cystic fibrosis. *Nature* 2001; **410**: 94-97
- 7 **Ahn W**, Kim KH, Lee JA, Kim JY, Choi JY, Moe OW, Milgram SL, Muallem S, Lee MG. Regulatory interaction between the cystic fibrosis transmembrane conductance regulator and  $\text{HCO}_3^-$  salvage mechanisms in model systems and the mouse pancreatic duct. *J Biol Chem* 2001; **276**: 17236-17243
- 8 **Lee MG**, Ahn W, Choi JY, Luo X, Seo JT, Schultheis PJ, Shull GE, Kim KH, Muallem S.  $\text{Na}^+$ -dependent transporters mediate  $\text{HCO}_3^-$  salvage across the luminal membrane of the main pancreatic duct. *J Clin Invest* 2000; **105**: 1651-1658
- 9 **Park M**, Ko SB, Choi JY, Muallem G, Thomas PJ, Pushkin A, Lee MS, Kim JY, Lee MG, Muallem S, Kurtz I. The cystic fibrosis transmembrane conductance regulator interacts with and regulates the activity of the  $\text{HCO}_3^-$  salvage transporter human  $\text{Na}^+/\text{HCO}_3^-$  cotransport isoform 3. *J Biol Chem* 2002; **277**: 50503-50509
- 10 **Zhao H**, Star RA, Muallem S. Membrane localization of  $\text{H}^+$  and  $\text{HCO}_3^-$  transporters in the rat pancreatic duct. *J Gen Physiol* 1994; **104**: 57-85
- 11 **Chambers JA**, Harris A. Expression of the cystic fibrosis gene and the major pancreatic mucin gene, MUC1, in human ductal epithelial cells. *J Cell Sci* 1993; **105** (Pt 2): 417-422
- 12 **Schoumacher RA**, Ram J, Iannuzzi MC, Bradbury NA, Wallace RW, Hon CT, Kelly DR, Schmid SM, Gelder FB, Rado TA. A cystic fibrosis pancreatic adenocarcinoma cell line. *Proc Natl Acad Sci U S A* 1990; **87**: 4012-4016
- 13 **Shumaker H**, Amlal H, Frizzell R, Ulrich CD, Soleimani M. CFTR drives  $\text{Na}^+/\text{HCO}_3^-$  cotransport in pancreatic duct cells: a basis for defective  $\text{HCO}_3^-$  secretion in CF. *Am J Physiol* 1999; **276**: C16-C25
- 14 **Greeley T**, Shumaker H, Wang Z, Schweinfest CW, Soleimani M. Downregulated in adenoma and putative anion transporter are regulated by CFTR in cultured pancreatic duct cells. *Am J Physiol Gastrointest Liver Physiol* 2001; **281**: G1301-G1308
- 15 **Namkung W**, Lee JA, Ahn W, Han W, Kwon SW, Ahn DS, Kim KH, Lee MG.  $\text{Ca}^{2+}$  activates cystic fibrosis transmembrane

- conductance regulator- and  $\text{Cl}^-$ -dependent  $\text{HCO}_3^-$  transport in pancreatic duct cells. *J Biol Chem* 2003; **278**: 200-207
- 16 **Chan HC**, Law SH, Leung PS, Fu LX, Wong PY. Angiotensin II receptor type I-regulated anion secretion in cystic fibrosis pancreatic duct cells. *J Membr Biol* 1997; **156**: 241-249
- 17 **Cheng HS**, So SC, Law SH, Chan HC. Angiotensin II-mediated signal transduction events in cystic fibrosis pancreatic duct cells. *Biochim Biophys Acta* 1999; **1449**: 254-260
- 18 **Cheng HS**, Wong WS, Chan KT, Wang XF, Wang ZD, Chan HC. Modulation of  $\text{Ca}^{2+}$ -dependent anion secretion by protein kinase C in normal and cystic fibrosis pancreatic duct cells. *Biochim Biophys Acta* 1999; **1418**: 31-38
- 19 **Cheung CY**, Wang XF, Chan HC. Stimulation of  $\text{HCO}_3^-$  secretion across cystic fibrosis pancreatic duct cells by extracellular ATP. *Biol Signals Recept* 1998; **7**: 321-327
- 20 **Thomas JA**, Buchsbaum RN, Zimniak A, Racker E. Intracellular pH measurements in Ehrlich ascites tumor cells utilizing spectroscopic probes generated in situ. *Biochemistry* 1979; **18**: 2210-2218
- 21 **Hegyi P**, Rakonczay Z Jr, Gray MA, Argent BE. Measurement of intracellular pH in pancreatic duct cells: a new method for calibrating the fluorescence data. *Pancreas* 2004; **28**: 427-434
- 22 **Weintraub WH**, Machen TE. pH regulation in hepatoma cells: roles for Na-H exchange, Cl- $\text{HCO}_3^-$  exchange, and Na- $\text{HCO}_3^-$  cotransport. *Am J Physiol* 1989; **257**: G317-G327
- 23 **Inglis SK**, Finlay L, Ramminger SJ, Richard K, Ward MR, Wilson SM, Olver RE. Regulation of intracellular pH in Calu-3 human airway cells. *J Physiol* 2002; **538**: 527-539
- 24 **Dudeja PK**, Hafez N, Tyagi S, Gailey CA, Toofanfard M, Alrefai WA, Nazir TM, Ramaswamy K, Al-Bazzaz FJ. Expression of the Na $^+$ /H $^+$  and Cl $^-$ / $\text{HCO}_3^-$  exchanger isoforms in proximal and distal human airways. *Am J Physiol* 1999; **276**: L971-L978
- 25 **Dudeja PK**, Rao DD, Syed I, Joshi V, Dahdal RY, Gardner C, Risk MC, Schmidt L, Bavishi D, Kim KE, Harig JM, Goldstein JL, Layden TJ, Ramaswamy K. Intestinal distribution of human Na $^+$ /H $^+$  exchanger isoforms NHE-1, NHE-2, and NHE-3 mRNA. *Am J Physiol* 1996; **271**: G483-G493
- 26 **Zsembery A**, Strazzabosco M, Graf J.  $\text{Ca}^{2+}$ -activated Cl $^-$  channels can substitute for CFTR in stimulation of pancreatic duct bicarbonate secretion. *FASEB J* 2000; **14**: 2345-2356
- 27 **Lee MG**, Choi JY, Luo X, Strickland E, Thomas PJ, Muallem S. Cystic fibrosis transmembrane conductance regulator regulates luminal Cl $^-$ / $\text{HCO}_3^-$  exchange in mouse submandibular and pancreatic ducts. *J Biol Chem* 1999; **274**: 14670-14677
- 28 **Waisbren SJ**, Geibel JP, Modlin IM, Boron WF. Unusual permeability properties of gastric gland cells. *Nature* 1994; **368**: 332-335
- 29 **Bonanno JA**, Guan Y, Jelamskii S, Kang XJ. Apical and basolateral  $\text{CO}_2$ - $\text{HCO}_3^-$  permeability in cultured bovine corneal endothelial cells. *Am J Physiol* 1999; **277**: C545-C553
- 30 **Bollert P**, Peters T, von Engelhardt W, Gros G. Mass spectrometric determination of  $\text{HCO}_3^-$  permeability and carbonic anhydrase activity in intact guinea-pig colon epithelium. *J Physiol* 1997; **502** ( Pt 3): 679-691
- 31 **Ishiguro H**, Naruse S, Kitagawa M, Suzuki A, Yamamoto A, Hayakawa T, Case RM, Steward MC.  $\text{CO}_2$  permeability and bicarbonate transport in microperfused interlobular ducts isolated from guinea-pig pancreas. *J Physiol* 2000; **528** Pt 2: 305-315
- 32 **Ishiguro H**, Steward MC, Lindsay AR, Case RM. Accumulation of intracellular  $\text{HCO}_3^-$  by Na $^+$ / $\text{HCO}_3^-$  cotransport in interlobular ducts from guinea-pig pancreas. *J Physiol* 1996; **495** ( Pt 1): 169-178
- 33 **de Ondarza J**, Hootman SR. Confocal microscopic analysis of intracellular pH regulation in isolated guinea pig pancreatic ducts. *Am J Physiol* 1997; **272**: G124-G134
- 34 **Satoh H**, Moriyama N, Hara C, Yamada H, Horita S, Kunimi M, Tsukamoto K, Iso-O N, Inatomi J, Kawakami H, Kudo A, Endou H, Igarashi T, Goto A, Fujita T, Seki G. Localization of Na $^+$ - $\text{HCO}_3^-$  cotransporter (NBC-1) variants in rat and human pancreas. *Am J Physiol Cell Physiol* 2003; **284**: C729-C737
- 35 **Thevenod F**, Roussa E, Schmitt BM, Romero MF. Cloning and immunolocalization of a rat pancreatic Na $^+$  bicarbonate cotransporter. *Biochem Biophys Res Commun* 1999; **264**: 291-298
- 36 **Gross E**, Abuladze N, Pushkin A, Kurtz I, Cotton CU. The stoichiometry of the electrogenic sodium bicarbonate cotransporter pNBC1 in mouse pancreatic duct cells is 2  $\text{HCO}_3^-$ :1 Na $^+$ . *J Physiol* 2001; **531**: 375-382
- 37 **Novak I**, Greger R. Electrophysiological study of transport systems in isolated perfused pancreatic ducts: properties of the basolateral membrane. *Pflugers Arch* 1988; **411**: 58-68
- 38 **Novak I**, Christoffersen BC. Secretin stimulates  $\text{HCO}_3^-$  and acetate efflux but not Na $^+$ / $\text{HCO}_3^-$  uptake in rat pancreatic ducts. *Pflugers Arch* 2001; **441**: 761-771
- 39 **Marino CR**, Jeanes V, Boron WF, Schmitt BM. Expression and distribution of the Na $^+$ - $\text{HCO}_3^-$  cotransporter in human pancreas. *Am J Physiol* 1999; **277**: G487-G494
- 40 **Scozzafava A**, Briganti F, Ilies MA, Supuran CT. Carbonic anhydrase inhibitors: synthesis of membrane-impermeant low molecular weight sulfonamides possessing in vivo selectivity for the membrane-bound versus cytosolic isozymes. *J Med Chem* 2000; **43**: 292-300
- 41 **Dahl NK**, Jiang L, Chernova MN, Stuart-Tilley AK, Shmukler BE, Alper SL. Deficient  $\text{HCO}_3^-$  transport in an AE1 mutant with normal Cl $^-$  transport can be rescued by carbonic anhydrase II presented on an adjacent AE1 protomer. *J Biol Chem* 2003; **278**: 44949-44958
- 42 **Sterling D**, Reithmeier RA, Casey JR. A transport metabolon. Functional interaction of carbonic anhydrase II and chloride/bicarbonate exchangers. *J Biol Chem* 2001; **276**: 47886-47894
- 43 **Sterling D**, Alvarez BV, Casey JR. The extracellular component of a transport metabolon. Extracellular loop 4 of the human AE1 Cl $^-$ / $\text{HCO}_3^-$  exchanger binds carbonic anhydrase IV. *J Biol Chem* 2002; **277**: 25239-25246
- 44 **Vince JW**, Reithmeier RA. Carbonic anhydrase II binds to the carboxyl terminus of human band 3, the erythrocyte Cl $^-$ / $\text{HCO}_3^-$  exchanger. *J Biol Chem* 1998; **273**: 28430-28437
- 45 **Sterling D**, Brown NJ, Supuran CT, Casey JR. The functional and physical relationship between the DRA bicarbonate transporter and carbonic anhydrase II. *Am J Physiol Cell Physiol* 2002; **283**: C1522-C1529
- 46 **Alvarez BV**, Loiseau FB, Supuran CT, Schwartz GJ, Casey JR. Direct extracellular interaction between carbonic anhydrase IV and the human NBC1 sodium/bicarbonate co-transporter. *Biochemistry* 2003; **42**: 12321-12329
- 47 **Hewett-Emmett D**. Evolution and distribution of the carbonic anhydrase gene families. *EXS* 2000; 29-76
- 48 **Nishimori I**, Fujikawa-Adachi K, Onishi S, Hollingsworth MA. Carbonic anhydrase in human pancreas: hypotheses for the pathophysiological roles of CA isozymes. *Ann N Y Acad Sci* 1999; **880**: 5-16
- 49 **Mahieu I**, Becq F, Wolfensberger T, Gola M, Carter N, Hollande E. The expression of carbonic anhydrases II and IV in the human pancreatic cancer cell line (Capan 1) is associated with bicarbonate ion channels. *Biol Cell* 1994; **81**: 131-141
- 50 **Fanjul M**, Salvador C, Alvarez L, Cantet S, Hollande E. Targeting of carbonic anhydrase IV to plasma membranes is altered in cultured human pancreatic duct cells expressing a mutated ( $\Delta$ F508) CFTR. *Eur J Cell Biol* 2002; **81**: 437-447
- 51 **Kivela AJ**, Parkkila S, Saarnio J, Karttunen TJ, Kivela J, Parkkila AK, Pastorekova S, Pastorek J, Waheed A, Sly WS, Rajaniemi H. Expression of transmembrane carbonic anhydrase isoenzymes IX and XII in normal human pancreas and pancreatic tumours. *Histochem Cell Biol* 2000; **114**: 197-204
- 52 **Cheng HS**, Leung PY, Cheng Chew SB, Leung PS, Lam SY, Wong WS, Wang ZD, Chan HC. Concurrent and independent  $\text{HCO}_3^-$  and Cl $^-$  secretion in a human pancreatic duct cell line (CAPAN-1). *J Membr Biol* 1998; **164**: 155-167
- 53 **Roch B**, Baro I, Hongre AS, Escande D. ATP-sensitive K $^+$  channels regulated by intracellular  $\text{Ca}^{2+}$  and phosphorylation in normal (T84) and cystic fibrosis (CFPAC-1) epithelial cells. *Pflugers Arch* 1995; **429**: 355-363
- 54 **Fong P**, Argent BE, Guggino WB, Gray MA. Characterization of vectorial chloride transport pathways in the human pancreatic duct adenocarcinoma cell line HPAF. *Am J Physiol Cell*

- Physiol* 2003; **285**: C433-C445
- 55 **Stuenkel EL**, Machen TE, Williams JA. pH regulatory mechanisms in rat pancreatic ductal cells. *Am J Physiol* 1988; **254**: G925-G930
- 56 **Novak I**, Hug M, Greger R. Intracellular pH in rat pancreatic ducts. *Comp Biochem Physiol A Physiol* 1997; **118**: 409-411
- 57 **Marteau C**, Silviani V, Ducroc R, Crotte C, Gerolami A. Evidence for apical Na<sup>+</sup>/H<sup>+</sup> exchanger in bovine main pancreatic duct. *Dig Dis Sci* 1995; **40**: 2336-2340
- 58 **Villanger O**, Veel T, Raeder MG. Secretin causes H<sup>+</sup>/HCO<sub>3</sub><sup>-</sup> secretion from pig pancreatic ductules by vacuolar-type H<sup>+</sup>-adenosine triphosphatase. *Gastroenterology* 1995; **108**: 850-859
- 59 **Ko SB**, Zeng W, Dorwart MR, Luo X, Kim KH, Millen L, Goto H, Naruse S, Soyombo A, Thomas PJ, Muallem S. Gating of CFTR by the STAS domain of SLC26 transporters. *Nat Cell Biol* 2004; **6**: 343-350
- 60 **Ishiguro H**, Steward MC, Sohma Y, Kubota T, Kitagawa M, Kondo T, Case RM, Hayakawa T, Naruse S. Membrane potential and bicarbonate secretion in isolated interlobular ducts from guinea-pig pancreas. *J Gen Physiol* 2002; **120**: 617-628

S- Editor Kumar M and Guo SY L- Editor Elsevier HK E- Editor Liu WF